Thermal Structure [National Oceanic and Atmospheric Administration (NOAA) Atlas Series, Government Printing Office, Washington, DC, in press].

3. Station OWS C was located (52.75°N, 35.5°W) in the subarctic gyre of the North Atlantic. This location is just north of the Ocean Polar Front, an upper ocean feature associated with the North Atlantic Current. From 1946 to 1973, OWS C was occupied by ships of the U.S. Coast Guard. From 1946 to 1964, temperature profiles were measured with MBT instruments. From 1964 through 1973, hydrographic casts (reversing thermometers to measure temperature and seawater samples gathered for salinity determinations) were made as well as MBT casts [see L. J. Hannon, "North Atlantic Ocean Station Charlie Terminal Report 1964–1973" (*Oceanographic Report CG 373–79*, U.S. Coast Guard Oceanographic Unit, Washington, DC, 1973)]. From 1975 through 1990, research ships from the former Soviet Union occupied this station. They took Nansen casts and salinity-temperature-depth profiles, in addition to some MBT profiles. Some of the former Soviet Union data taken at OWS C were available only in the form of daily means. Therefore, we averaged all data to obtain daily means before forming other averages so as to utilize all the former Soviet Union data and analyze all data in a consistent manner.
4. S. Levitus and T. P. Boyer, *World Ocean Atlas 1994*, vol. 4: *Temperature* (NOAA Atlas NESDIS 4, Government Printing Office, Washington, DC, 1994).
5. H. H. Harman, *Modern Factor Analysis* (Univ. of Chicago Press, Chicago, ed. 3, 1976); J. E. Jackson, *A User's Guide to Principal Components* (Wiley, New York, 1991).
6. J. R. N. Lazier, *Atmos. Ocean* **18**, 227 (1980); *Deep-Sea Res.* **35**, 1247 (1988); in *Decadal-Scale Variability of the North Atlantic Ocean*, K. Bryan, Ed. (National Academy Press, Washington, DC, in press).
7. P. G. Brewer *et al.*, *Science* **222**, 1237 (1983).
8. A. H. Taylor, *J. Climatol.* **3**, 253 (1983).
9. H. D. Dooley, J. H. A. Martin, D. J. Ellet, *Rapp. P.V. Reun. Cons. Int. Explor. Mer* **185**, 179 (1984).
10. D. Roemmich and C. Wunsch, *Nature* **307**, 447 (1984).
11. D. Roemmich, in *Glaciers, Ice Sheets, and Sea Level: Effect of a CO_2-Induced Climatic Change* (Department of Energy, Washington, DC, 1985), pp. 104–115.
12. J. H. Swift, in *Climatic Processes and Climate Sensitivity* (*Geophys. Monogr. Ser. 29*), J. E. Hansen and T. Takahashi, Eds. (American Geophysical Union, Washington, DC, 1984), pp. 39–47; in *Glaciers, Ice Sheets, and Sea Level: Effect of a CO_2-Induced Climatic Change* (Department of Energy, Washington, DC, 1985), pp. 129–138.
13. R. Dickson, J. Meinke, S. A. Malmberg, A. J. Lee, *Progr. Oceanogr.* **20**, 103 (1988).
14. J. Antonov and P. Groisman, *Meteorol. Hydrol.* **3**, 57 (1988) (in Russian).
15. S. Levitus, *J. Geophys. Res.* **94**, 6091 (1989); *ibid.*, p. 9679; *ibid.*, p. 16125; *ibid.* **95**, 5233 (1990).
16. J. Antonov, *Meteorol. Hydrol.* **4**, 78 (1990) (in Russian); J. Antonov, *J. Climate* **6**, 1928 (1993).
17. D. R. Cayan, *J. Phys. Oceanogr.* **22**, 859 (1992).
18. Funding for this work was provided by the NOAA Climate and Global Change Program and the NOAA Environmental Sciences Data and Information Management Program. This work was completed while J.A. was a research associate (National Research Council) at the National Oceanographic Data Center, NOAA, Washington, DC.

20 June 1994; accepted 18 August 1994

Atomic-Scale Dynamics of a Two-Dimensional Gas-Solid Interface

S. J. Stranick, M. M. Kamna, P. S. Weiss*

The interface between a two-dimensional (2D) molecular gas and a 2D molecular solid has been imaged with a low-temperature, ultrahigh-vacuum scanning tunneling microscope. The solid consists of benzene molecules strongly bound to step edges on a Cu{111} surface. Benzene molecules on the Cu{111} terraces move freely as a 2D gas at 77 kelvin. Benzene molecules transiently occupy well-defined adsorption sites at the 1D edge of the 2D solid. Diffusion of molecules between these sites and exchange between the two phases at the interface are observed. On raised terraces of the copper surface, the 2D gas is held in a cage of the solid as in a 2D nanometer-scale gas bulb.

The 2D phase diagram for adsorbates on surfaces has all of the complexity of the more familiar 3D analogs. Adsorbates can be found as 2D gases, liquids, and solids. Different 2D structures are formed as temperature and coverage are varied. A variety of scattering and diffraction techniques have been used to study the phase transitions of 2D systems (*1*). We report here observations of the atomic-scale dynamics of the equilibrium at the interface between a 2D solid and a 2D gas. We can record the motion of individual molecules at this interface, as has never been possible for 3D systems. We used a low-temperature, ultrahigh-vacuum (UHV) scanning tunneling microscope (STM) (*2*) to observe these dynamics for benzene molecules adsorbed on the Cu{111} surface.

The STM has been used to analyze the kinetics of motion of surface adsorbates and surface features such as steps and vacancies (*3*–*6*). In making these measurements, researchers have used many of the methods earlier developed for quantifying motion on the atomic scale by field ion microscopy (*7*). For STM measurements, correlation techniques have been used to analyze images of mobile adsorbates at high surface coverages to determine favored adsorption sites, surface ordering, and interaction energies (*8*).

Weiss and Eigler have studied adsorption sites and their effects on STM images of isolated benzene molecules on Pt{111} at 4 K (*9*). At such a low temperature, benzene is frozen in place and no motion is observed. Benzene molecules have also been imaged on Rh{111} at room temperature when held fixed in various ordered overlayers by coadsorbed CO (*10*). On both Pt{111} and Rh{111} surfaces, benzene molecules lie flat, that is, with the molecular plane parallel to the surface plane. In another study of surface motion, Wolkow and Schofield used a low-temperature STM to observe the diffusion and perhaps desorption into the vacuum of isolated benzene molecules on the Si{111} surface (*11*).

After initial electrochemical polishing and repeated sputtering and annealing cycles in UHV, we obtained a clean flat Cu{111} crystal surface. We dosed the freshly cleaned crystal to saturation coverage at room temperature by bleeding a small amount of benzene gas through a sapphire leak valve into the vacuum chamber. We checked the purity of the benzene in situ by mass spectroscopy to verify that impurities and undesired wall reactions were negligible. After dosing, the room-temperature Cu{111} sample was rapidly transferred to a cryogenic UHV STM chamber held at 77 or 4 K (*2*).

Earlier studies by Bent and co-workers have shown that benzene adsorbs and desorbs molecularly on the Cu{111} surface (*12*). As for the close-packed Pt{111} and Rh{111} surfaces, the first monolayer of benzene adsorbs with the molecular plane parallel to the surface plane (*12*). From temperature-programmed desorption (TPD) of perdeutero (d_6–) benzene on Cu{111}, multilayer and monolayer coverages of benzene are known to desorb from the surface below 250 K. A high-temperature tail in the TPD spectrum extending to 300 K is attributed to desorption from surface defect sites. Therefore, by dosing the Cu{111} crystal at room temperature with benzene, we preferentially populated defect sites such as step edges on the surface.

Initial STM observations showed that at both 4 and 77 K, the monatomic step edges on the Cu{111} surface were indeed decorated by adsorbed benzene. These features were not present in STM images of the bare Cu{111} surface. STM images of the benzene-covered surface recorded at 77 K are shown in Fig. 1, A and B. Both straight and meandering monatomic height steps are present on the Cu{111} surface (*13*), and all are decorated with benzene molecules. Because along straight steps benzene molecules order into well-defined adsorption sites, we concentrated our analysis on these step configurations.

At 77 K the benzene molecules are mo-

Department of Chemistry, Pennsylvania State University, University Park, PA 16802, USA.

*To whom correspondence should be addressed.

bile on the terraces. At 4 K, as on Pt{111} (*9*), molecular diffusion is frozen out on the terraces as well, and for our method of dosing the surface coverage of benzene on the Cu{111} terraces (>200 Å wide) is ~0.002 monolayer (*14*). That molecules stick at the step edges is not surprising (*15*). Even rare gases such as Xe preferentially bind to step edges on crystal surfaces (*16*). For benzene, the stronger interactions of the molecules with adsorption sites along substrate steps lead to the formation of a fixed 2D solid at these sites. At 77 K, benzene molecules remain mobile on the atomically flat terraces of Cu{111} and behave as a 2D gas in dynamic equilibrium with the 2D molecular solid along the step edges. This behavior at the interface is analogous to the behavior of solutions at electrode surfaces where at the metal-solution interface there exists a bound, "specifically adsorbed" layer of solution that contributes to the double layer (*17*). It is believed that at the metal-solution interface the molecules from the solution are able to change places with this bound layer. We observed an analogous situation in two dimensions on the surface of our Cu{111} crystal.

Initial STM images of straight Cu steps on benzene-dosed Cu{111} at 77 K revealed that there are two rows of benzene adsorbed at the step (Fig. 1B). A well-defined row of benzene molecules lies below the step riser (indicated by arrow 1), and another lies above the step riser (indicated by arrow 2). These first two rows are held rigidly in place and form a 2D solid of benzene molecules at the Cu{111} step edge. In addition, a "noisy" (or "phantom") line of molecules is adjacent to row 2 on the upper terrace (indicated by arrow 3). We attribute the instability in row 3 to molecules moving in and out of the preferred sites of this row. The molecules can move parallel to the interface (along row 3) or can desorb into the 2D molecular gas on the terrace and readsorb, thus setting up the dynamic equilibrium between the two phases.

The positions of the benzene molecules correspond to a 2× (with twice the copper atomic lattice spacing) solid parallel to the straight step edges with respect to the underlying Cu{111} lattice. We determined the spacing between molecules by imaging the Cu{111} lattice. Given the low surface corrugation of close-packed noble metal surfaces, imaging of the lattice atoms is challenging but can be accomplished if a benzene molecule is lifted onto the STM tip (*18*) and used as a "Behm amplifier" (*19*, *20*). Imperfections such as kinks in the straight step edges of the Cu{111} substrate are accommodated by defects formed in the 2D benzene solid. As noted below, molecules at these defect sites have different binding energies and thus move at different rates than molecules in the perfectly ordered 2D solid. The benzene molecules adsorbed on meandering Cu{111} step edges most often form disordered 2D solids.

The growth of C_{60} films on the Cu{111} and other noble metal surfaces has also been shown to proceed from step edges (*21*). The step edges for C_{60} and for benzene function as atomic-scale nucleation sites, much as a macroscopic scratch in the bottom of a beaker serves to nucleate the precipitation of crystals out of a supersaturated solution.

We analyzed the STM images to determine the fraction of time that the features attributed to the molecules are present in row 3. We set a threshold level in the topography at two-thirds the half maximum of a typical molecular feature. We recorded the fraction of the total number of pixels within the half width at half maximum of the center of the adsorption site that are above this threshold level (*22*). Analyses of rows 1 and 2 indicated occupations of 0.99 ± 0.01 and 0.99 ± 0.02, respectively. The row 3 adsorption sites chosen for analysis were determined as described below. Analysis of these "next" adsorption sites along row 3 indicated a fractional occupation of 0.09 ± 0.08 so long as the bias voltage was kept low (that is, at nonperturbing values), 0.05 V $\lesssim |V_{\mathrm{tip}}| \lesssim$ 0.5 V for tunneling currents, I, of 100 pA. We determined this range of tunneling conditions by analyzing the distributions of times the molecules spend at the transiently occupied adsorption sites as a function of tunneling parameters and of scanning direction, rate, and resolution. For nonperturbing tunneling conditions these distributions are independent of scan rate and resolution, and we found that molecules at sites along row 3 have mean occupation times of ~7 ms (*23*).

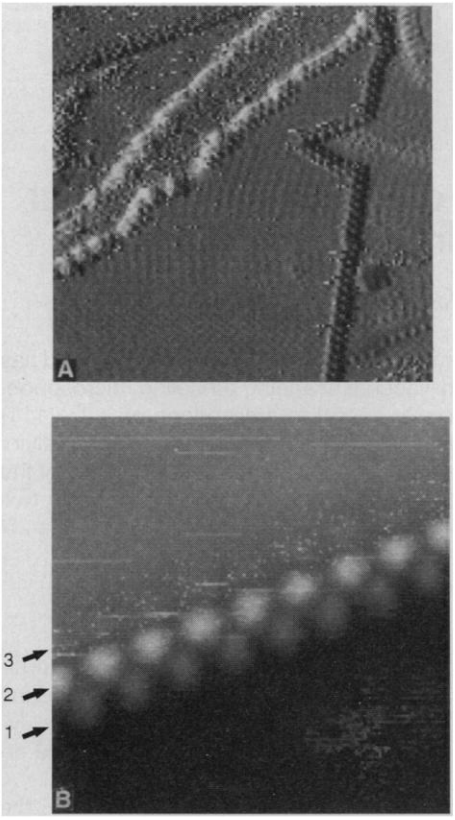

Fig. 1. Scanning tunneling microscope images showing a Cu{111} surface with adsorbed benzene molecules. The molecules decorate the step edges in the form of a 2D solid. The images were recorded at 77 K in constant-current mode. All images are unfiltered and were recorded at a tunneling current of 100 pA and a tip bias voltage of −0.1 V. (**A**) A 200 by 200 Å area showing straight and meandering substrate steps with the derivative along the horizontal axis displayed (as if the surface is illuminated from the left). (**B**) A topographic display of a 40 by 40 Å area showing a decorated straight step edge.

On raised terraces on the Cu{111} surface—mesas—the encircling 2D solid benzene confines the 2D molecular gas. Such a mesa is shown in the 50 by 30 Å area of the Cu surface in Fig. 2, also recorded at 77 K. The solid benzene circles the mesa. The 2D gas molecules can slide back and forth on the mesa faster than the time scale of the STM imaging the surface. This phenomenon is the 2D equivalent of a gas bulb 30 Å long. Entrapping this 2D molecular gas will make possible independent study of these trapped molecules and their interactions with each other and with the tunneling electrons supplied by the STM tip. Beebe and co-workers recently found that organic liquids can be entrapped in nanometer-size etch pits in graphite and that an STM can be used to study these liquids as independent collections of molecules, but in that case molecules could still interact and exchange with the organic liquid overlayer (*24*).

If perturbing bias voltages are reached

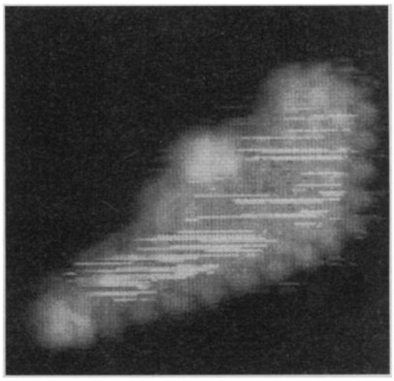

Fig. 2. An STM image showing a 50 by 30 Å area of a Cu{111} surface recorded at 77 K that includes a triangular mesa one atom higher than the surrounding terrace and approximately 30 Å long. The molecules of the 2D solid entrap the 2D gas. The gas molecules are apparent as streaks in the interior area of the mesa.

($|V_{\mathrm{tip}}| \gtrsim 0.9$ V for tunneling currents, I, of 100 pA at 77 K), the images of step edges are changed. Once this threshold is exceeded, the STM tip sweeps additional molecules to the edge of the molecular solid on the upper terrace above the step riser (if these are within the field imaged in the STM scan). At this point, we find row 3 substantially occupied and a fourth row becomes fractionally occupied (Fig. 3A). A cross-sectional view along these rows (Fig. 3B) highlights the stability of rows 1 and 2 and the noise inherent in row 3. As can be seen in Fig. 3A, the molecules are often present for several line scans (horizontal in the image) and then disappear and reappear on the time scale of imaging (seconds per line scan). The partially occupied sites now evident in row 3 are those that were used for the analysis of the unperturbed interface above.

After molecules have been moved to the step edge, we can again analyze the occupation of the sites along the step edges using nonperturbing tunneling conditions. Inspection of images such as the one shown in Fig. 3A reveals that a fourth row is also present for a smaller fraction of the time. The occupation fractions at the edge of the 2D solid after molecules have been swept to the step edge are 1.00 ± 0.01 for row 1, 0.97 ± 0.04 for row 2, 0.76 ± 0.10 for row 3, and 0.07 ± 0.02 for row 4. For nonperturbing tunneling conditions after molecules have been swept to the step edge, molecules at sites along row 3 have mean occupation times in single adsorption sites of ~20 ms and those along row 4 have mean occupation times of ~10 ms (*23*).

The outermost row has comparable density, if it is attached to row 2 before molecules have been swept to the step edge or if it is attached to row 3 afterward. This is an indication that the interactions that cause 2D gas molecules to adsorb at the interfaces with the 2D solid are intermolecular rather than due to the proximity of the step edge. Further evidence for this type of interaction comes from close examination of the perturbations of the surface electronic structure by the step edge (*25*) and by the molecules. Low-temperature STM measurements may shed light on these electronic interactions that account for the adsorption sites along step edges (*26*).

STM images of the step edges adjacent to where molecules were deliberately added also show increased coverage, a strong indication that motion parallel to the step edge—diffusion of molecules between interface sites—is facile. The decay rate for the increased occupation of rows 3 and 4 after molecules are swept there, the desorption rate, is much longer (time scale of more than 1 hour). Thus, just as is typical for adsorbates on the surface of a 3D solid (*27*), diffusion along the 1D edge of the 2D solid is substantially faster than desorption from the interface sites into the 2D gas on the terraces. At special sites such as kinks in the substrate step edges where the benzene molecules are more weakly bound, this situation can be reversed and we can observe adsorption-desorption with no apparent lateral diffusion along the interface. Discriminating between the dynamics of the great variety of surface sites in this manner is only possible because of our ability to focus observations on these sites independently with the atomic-scale view of the STM.

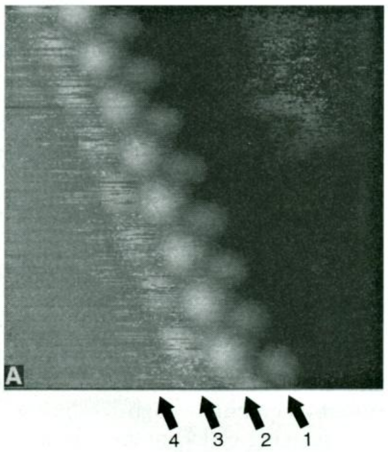

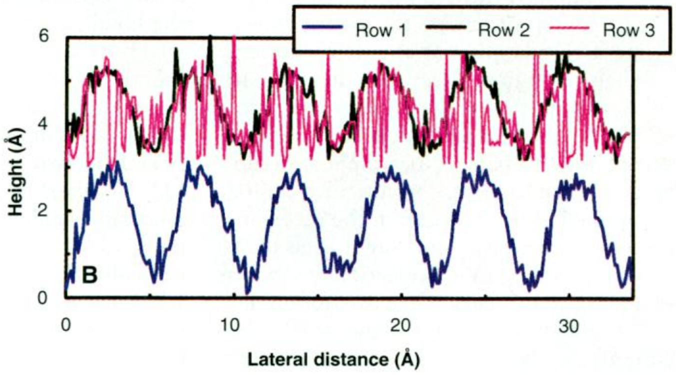

Fig. 3. (**A**) An STM image recorded at 77 K of the 40 by 40 Å area shown in Fig. 1B (but rotated 90°) after the STM tip has intentionally swept additional molecules from the terrace to fill adsorption sites above the step riser. Two rows of benzene (rows 3 and 4) now transiently occupy sites on the upper terrace adjacent to the 2D molecular benzene solid. (**B**) Cross sections along the rows marked in (A) show the static occupation of the sites in rows 1 and 2, above and below the step riser, respectively. Molecules in row 3 undergo motion that is fast on the time scale of STM imaging (seconds). This fast time scale can be seen from the rapid oscillation of the cross section for row 3 between topographic heights typical of occupied and unoccupied surface sites. Row 2 data are shifted by one-half in intermolecular spacing so as to align molecular features for all three rows.

REFERENCES AND NOTES

1. See, for example, B. Pluis, A. W. Denier van der Gon, J. W. M. Frenken, J. F. Van der Veen, *Phys. Rev. Lett.* **59**, 2678 (1987); K. Kern, R. David, P. Zeppenfeld, G. Comsa, *Surf. Sci.* **195**, 353 (1988).
2. S. J. Stranick, M. M. Kamna, P. S. Weiss, *Rev. Sci. Instrum.* **65**, 3211 (1994).
3. G. Binnig, H. Fuchs, E. Stoll, *Surf. Sci. Lett.* **169**, L295 (1986).
4. M. G. Lagally, *Phys. Today* **46** (no. 11), 24 (1993).
5. D. J. Trevor, C. E. D. Chidsey, D. N. Loiacono, *Phys. Rev. Lett.* **62**, 929 (1989).
6. Y. W. Mo, J. Kleiner, M. B. Webb, M. G. Lagally, *ibid.* **66**, 1998 (1991).
7. T. T. Tsong, *Surf. Sci. Rep.* **8**, 127 (1988); G. Ehrlich and K. Stolt, *Annu. Rev. Phys. Chem.* **31**, 603 (1980).
8. J. C. Dunphy, P. Sautet, D. F. Ogletree, O. Dabboussi, M. B. Salmeron, *Phys. Rev. B* **47**, 2320 (1993); J. C. Dunphy, P. Sautet, D. F. Ogletree, M. B. Salmeron, *J. Vac. Sci. Technol. A* **11**, 2145 (1993).
9. P. S. Weiss and D. M. Eigler, *Phys. Rev. Lett.* **71**, 3139 (1993).
10. H. Ohtani, R. J. Wilson, S. Chiang, C. M. Mate, *ibid.* **60**, 2398 (1988); S. Chiang, R. J. Wilson, C. M. Mate, H. Ohtani, *J. Microsc.* (*Oxford*) **152**, 567 (1988); *Vacuum* **41**, 118 (1990).
11. R. Wolkow and J. A. Schofield Jr., *AT&T Bell Lab. Tech. Mem. 11541-921204-76TM* (1992) and *11541-921204-77TM* (1992).
12. M. Xi and B. E. Bent, *J. Vac. Sci. Technol. B* **10**, 2440 (1992); M. Xi, M. X. Yang, S. K. Jo, B. E. Bent, P. Stevens, *J. Chem. Phys.*, in press.
13. The straight steps have two different orientations: close-packed steps oriented in the $\langle 11\bar{2}\rangle$ direction and microfacets of Cu{100} oriented nominally in the $\langle 0\bar{1}1\rangle$ direction.
14. Because the mobility of molecules on terraces freezes out below 77 K, the equilibrium population of molecules on terraces may be lower at this "freeze-out" temperature. Nevertheless, the benzene coverage on Cu{111} terraces at 4 and 77 K is very low with our deposition method.
15. J. A. Serri, M. J. Cardillo, G. E. Becker, *J. Chem. Phys.* **77**, 2175 (1982); G. A. Somorjai, *Chemistry in Two Dimensions: Surfaces* (Cornell Univ. Press, Ithaca, NY, 1981); S. C. Wang and G. Ehrlich, *Phys. Rev. Lett.* **70**, 41 (1993).
16. P. S. Weiss and D. M. Eigler, *Phys. Rev. Lett.* **69**, 2240 (1992).
17. A. J. Bard and L. R. Faulkner, *Electrochemical Methods: Fundamentals and Applications* (Wiley, New York, 1980).
18. P. S. Weiss and D. M. Eigler, in *Nanosources and Manipulations of Atoms Under High Fields and Temperatures: Applications*, Vu Thien Binh, N. Garcia, K. Dransfeld, Eds., vol. 235 of NATO Advanced Study Institutes Series (Kluwer Academic, Dordrecht, Netherlands, 1993), p. 213.
19. J. Wintterlin *et al.*, *Phys. Rev. Lett.* **62**, 59 (1989).
20. With a molecule on the STM tip acting to enhance the measured corrugation of the close-packed face-centered-cubic lattice, it remains unclear if the peaks of the measured corrugation correspond to the substrate atom positions. Therefore, this method does

not allow us to determine the adsorption sites of the molecules.
21. K. Motai *et al.*, *Jpn. J. Appl. Phys.* **32**, L450 (1993); E. I. Altman and R. J. Colton, *Surf. Sci.* **295**, 13 (1993).
22. This method reduces the contribution of noise in imaging, as the tip displacements are well under the (1/6 maximum) difference between the 1/3 maximum threshold value and the half maximum at the perimeter of the area analyzed. The uncertainties reported are one standard deviation when tens of observations of each equivalent site are averaged. The occupation fractions measured are not particularly sensitive to the choice of areas and thresholds, so long as the STM topography due to a benzene molecule would be higher than the threshold for the area selected.
23. We do not have sufficient statistics to determine the order of these kinetics. Further, once the tunneling conditions are found that do not perturb the motion of the molecules, one can measure the occupation of the sites to much shorter times by following the tunneling current when the tip is kept fixed at the adsorption site.
24. D. L. Patrick, V. J. Cee, T. P. Beebe Jr., *Science* **265**, 231 (1994).
25. M. F. Crommie, C. P. Lutz, D. M. Eigler, *Nature* **363**, 524 (1993); Y. Hasegawa and Ph. Avouris, *Phys. Rev. Lett.* **71**, 1071 (1993); Ph. Avouris and I.-W. Lyo, *Science* **264**, 942 (1994).
26. M. M. Kamna, S. J. Stranick, P. S. Weiss, in preparation.
27. S. J. Lombardo and A. T. Bell, *Surf. Sci. Rep.* **13**, 1 (1991); D. L. Meixner and S. M. George, *J. Chem. Phys.* **98**, 9115 (1993).
28. We thank B. Bent, M. Cole, E. Heller, and H. Rohrer for helpful discussions. This research was supported by the National Science Foundation Chemistry and Presidential Young Investigator programs, the Office of Naval Research, AT&T Bell Laboratories, the Biotechnology Research and Development Corporation, Eastman Kodak, and Hewlett-Packard. S.J.S. thanks the Shell Foundation for a graduate fellowship.

6 June 1994; accepted 9 August 1994

Direct Determination of Grain Boundary Atomic Structure in $SrTiO_3$

M. M. McGibbon,* N. D. Browning, M. F. Chisholm,
A. J. McGibbon, S. J. Pennycook, V. Ravikumar, V. P. Dravid

An atomic structure model for a 25° [001] symmetric tilt grain boundary in $SrTiO_3$ has been determined directly from experimental data with the use of high-resolution *Z*-contrast imaging coupled with electron energy loss spectroscopy. The derived model of the grain boundary was refined by bond-valence sum calculations and reveals candidate sites for dopant atoms in the boundary plane. These results show how the combined techniques can be used to deduce the atomic structure of defects and interfaces without recourse to preconceived structural models or image simulations.

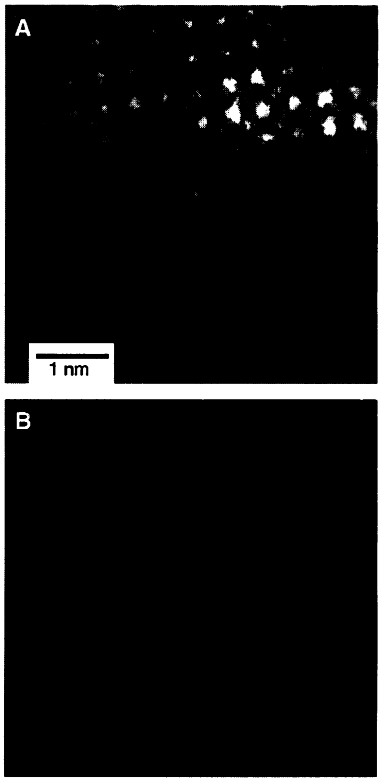

Fig. 1. (**A**) *Z*-contrast image of a 25° [001] tilt boundary in an $SrTiO_3$ bicrystal, with (**B**) the maximum entropy object function providing scattering intensities and coordinates of the Sr and Ti atomic columns directly from the image.

Internal interfaces, such as grain boundaries, have a pervasive influence on a variety of macroscopic properties and phenomena (*1*). Although it is well accepted that the atomic structure of interfaces does dictate the behavior of the bulk, the details of this relation are far from clear. One such model electroceramic system in which grain boundary phenomena control a variety of electrical properties, such as nonlinear current-voltage characteristics (*2*, *3*) is $SrTiO_3$. The explanation for the electrical activity of grain boundaries is largely phenomenological, and there is considerable debate whether the electrical properties can be rationalized in terms of acceptor states at the grain boundary core (*4*–*6*). Thus, determining the atomic structure-property relation for individual grain boundaries in such systems is of considerable significance (*7*, *8*). As a first step toward this goal, we have initiated a study of $SrTiO_3$ bicrystals that limits the number of degrees of freedom associated with the interface and provides a realistic opportunity to probe the structure-property relation for single isolated boundaries (*9*).

To determine the atomic and electronic structure of the grain boundary on an atomic scale, a technique is required that probes both composition and chemical bonding with atomic resolution. Here we present a detailed atomic structure model for an undoped grain boundary in $SrTiO_3$, made possible by combining high-resolution Z-contrast imaging to locate the cation columns at the boundary, with simultaneous electron energy loss spectroscopy to examine light-element coordination at atomic resolution.

High-resolution Z-contrast imaging in the scanning transmission electron microscope (STEM) provides an incoherent image in which changes in atomic structure and composition across an interface can be interpreted directly without the need for preconceived atomic structure models (*10*). Provided the incident electron probe is smaller than the lattice spacing (for a sample oriented to a major zone axis), the current can be channeled along a single atomic column. Because the probe is scanned, the resultant image is a map of the columnar scattering power that in turn depends on the atomic number, Z, of each column. The spatial resolution is primarily limited by the probe size of the STEM [2.2 Å in our case, using a VG Microscopes HB501UX (Sussex, United Kingdom)] because beam spreading is reduced, even in thicker samples, by the channeling effect (*11*, *12*). Because the Z-contrast image is formed by electrons scattered through high angles, parallel detection electron energy loss spectroscopy (PEELS) can be used simultaneously to provide complementary chemical information on an atomic scale (*13*, *14*). The fine structure in the energy loss spectra can be used to investigate the local electronic structure and the nature of the bonding across the interface (*15*, *16*).

The power of combining Z-contrast imaging and PEELS to solve the atomic and chemical structure of grain boundaries is demonstrated here in the study of an undoped $SrTiO_3$ bicrystal purchased from Shinkosha, Ltd., Tokyo, Japan. Specimens with the boundary parallel to the beam direction were prepared for electron microscopy by mechanical polishing and ion-beam thinning. Figure 1A shows a Z-contrast image from a symmetric portion of a 25° [001] tilt boundary. At room temperature, $SrTiO_3$ has a cubic perov-

---

M. M. McGibbon, N. D. Browning, M. F. Chisholm, A. J. McGibbon, S. J. Pennycook, Solid State Division, Oak Ridge National Laboratory, Oak Ridge, TN 37831–6030, USA.
V. Ravikumar and V. P. Dravid, Northwestern University, Department of Materials Science and Engineering, Evanston, IL 60208, USA.

*To whom correspondence should be addressed.